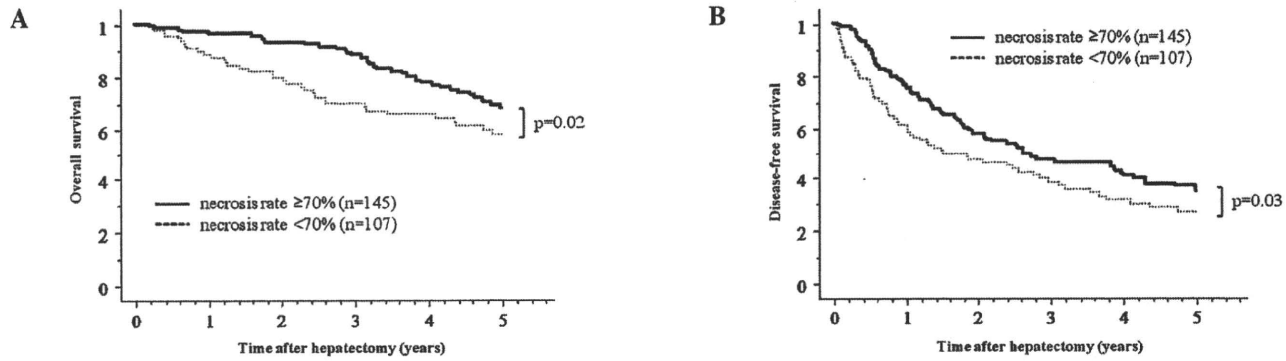

Figure 3. (A) Overall survival curve for the pre-operative TACE group according to the necrosis rate induced by TACE. (B) The 5-year overall and disease-free survival for necrosis rate ≥70% was better than that for necrosis rate <70% (p=0.02).

Table III. Clinicopathological characteristics of the pre-operative TACE and non-TACE groups with tumor size ≥5 cm in diameter.

Variable	Pre-operative TACE (n=83)	Non-TACE (n=47)	P-value
Age (years)	60.3±8.5	61.9±9.2	0.319
Gender (male/female)	71/12	37/10	0.304
HBs-Ag (+)	43	23	0.556
HCV-Ab (+)	28	19	0.575
Child-Pugh grade (A/B)	71/12	42/5	0.594
CLIP score (0/1-2/3-6)	32/44/7	15/26/6	0.632
Serum AFP (>5 ng/ml)	49	29	0.376
Serum PIVKA-II (>40 mAU/l)	52	28	0.270
Tumor size (cm)	7.9±3.5	9.6±13.8	0.281
Multiple tumor	36	22	0.585
Portal vein invasion (+)	10	8	0.414
Intrahepatic metastasis (+)	34	21	0.640
TNM stage (I/II/III/IV-A)	0/49/25/9	0/25/12/10	0.356

TACE, transcatheter arterial embolization; AFP, α-fetoprotein; PIVKA-II, protein induced by vitamin K antigen II. Data are expressed as the mean ± SD.

after hepatectomy compared to the non-TACE group (p=0.04) (Fig. 2), but no benefit in overall survival was noted (p=0.70). There was no difference in the clinicopathologic background between patients of the two groups with tumors ≥5 cm in diameter (Table III). Additionally, to evaluate the influence of tumor size, we divided patients into groups according to 1 cm differences in tumor diameter and analysed each group regarding survival; there were no significant benefits between groups except for neoplasms ≥5 cm. Analysis of sites of recurrence showed that 134 and 36 patients experienced intrahepatic and extrahepatic recurrence in the pre-operative TACE group, and 153 and 25 patients in the non-TACE group (p=0.09).

Effect of the rate of tumor cell necrosis on survival. To determine the prognostic importance of the extent of necrosis of the tumor after TACE, patients treated with pre-operative TACE were divided into two groups according to the degree of tumor necrosis, and survival was calculated. The results of the Kaplan-Meier method showed that the overall and disease-free survivals over 5 years after hepatectomy for patients with tumors showing ≥70% necrosis (n=145) were superior to those with <70% necrosis (n=107). The 1-, 3- and 5-year overall survival rates were 97.1, 88.2 and 68.2% for the ≥70% necrosis group, and 89.1, 70.3 and 58.1% for the <70% necrosis group, respectively (p=0.02) (Fig. 3). The 1-, 3- and 5-year disease-free survival rates were 75.5, 46.9 and 36.5% for the ≥70% necrosis group, and 60.8, 38.5 and 27.0% for the <70% necrosis group, respectively (p=0.03). Analysis of recurrence sites showed that 82 and 12 patients experienced intrahepatic and extrahepatic recurrence in the ≥70% tumor necrosis group, and 52 and 24 patients in the <70% tumor necrosis group (p<0.01).

Patients with HCCs ≥5 cm exhibited a benefit of pre-operative TACE for disease-free survival in our study. By contrast, the necrosis rate was another prognostic factor in overall and disease-free survival. Therefore, we performed another analysis for patients with HCCs ≥5 cm and ≥70% necrosis. A survival benefit was noted in both overall and disease-free survival for patients bearing ≥5 cm HCCs in the ≥70% necrosis group; the 5-year overall and disease-free

Table IV. Studies on pre-operative TACE for HCC.

Author (Refs.)	No. of patients*	Tumor factor	% Overall survival TACE vs. control (years)	% Disease-free survival TACE vs. control (years)	Result
Clinical trials					
Wu *et al* (20)	24:48	Ts ≥10 cm	32 vs. 60 (5)	40 vs. 50 (3)	Harmful
Yamasaki *et al* (21)	50:47	2≤ Ts ≤5 cm	63 vs. 62 (5)	39 vs. 31 (5)	NS
Zhou *et al* (22)	52:56	Ts ≥5 cm	31 vs. 21 (5)	13 vs. 9 (5)	NS
Peng *et al* (9)	51:53	Vp	21 vs. 8.5 (5)	NA	Effective
Zhong *et al* (11)	59:59	Stage IIIA	23 vs. 18 (5)	9 vs. 2 (5)	Effective
Retrospective studies					
Imaoka *et al* (17)	37:52	Ts <10 cm	NA	72 vs. 54 (2)	Effective
Monden *et al* (23)	71:21		63 vs. 62 (3)	NA	NS
Nagasue *et al* (27)	31:107		31 vs. 45 (3)	NA	NS
Adachi *et al* (18)	46:26	Ts ≤5 cm,Vp(-), Vv(-), IM(-)	NA	52 vs. 49 (3)	Effective (CN group)
Harada *et al* (15)	98:33		78 vs. 68 (3)	38 vs. 34 (3)	Effective (CN group)
Uchida *et al* (28)	60:68		61 vs. 73 (3)	57 vs. 48 (3)	Harmful
Majno *et al* (14)	49:27		57 vs. 47 (3)	33 vs. 22 (3)	Effective (downstage or CN group)
Paye *et al* (24)	24:24		62 vs. 65 (3)	32 vs. 16 (3)	NS
Di Carlo *et al* (13)	55:45	Ts ≤5 cm	70 vs. 38 (3)	40 vs. 20 (3)	Effective
Lu *et al* (12)	44:76		50 vs. 52 (3)	32 vs. 36 (3)	NS
	(24:57)	2≤ Ts ≤8 cm	42 vs. 61 (3)	21 vs. 43 (3)	NS
	(20:19)	Ts ≥8 cm	53 vs. 33 (3)	32 vs. 11 (3)	Effective
Zhang *et al* (19)	120:1337		NA	51 (n≥2) vs. 36 (n≥1) vs. 21 (control) (5)	Effective
Gerunda *et al* (16)	20:17	Ts ≤5 cm	43 vs. 38 (5)	57 vs. 21 (5)	Effective (DFS)
Sugo *et al* (10)	13:73		NA	46 vs. 39 (3)	NS
	(58:35)	Stage I, II	NA	NA	NS
	(55:38)	Stage III, IV	NA	41 vs. 21 (3)	Effective
Sasaki *et al* (25)	109:126		28 vs. 50 (5)	19 vs. 22 (5)	Harmful
Choi *et al* (26)	120:153		NA	51 vs. 47 (5)	NS
Lee *et al* (29)	114:236		47 vs. 52 (5)	29 vs. 36 (5)	Harmful

TACE, transcatheter arterial embolization; Ts, tumor size; Vp, portal vein invasion; Vv, hepatic vein invasion; IM, intrahepatic metastasis; NA, not available; CN, complete necrosis. *Patients that received to those that did not receive TACE.

survival rates were 63.9 and 41.0% (n=43), and for patients bearing ≥5 cm HCCs in the <70% necrosis group, 42.8 and 16.1% (n=40) (p=0.02 and p<0.01, respectively).

Changes in AFP mRNA in peripheral blood. Among the last 123 patients for whom serum AFP mRNA was measured pre-operatively, 13 (11.6%) were positive. There was a significant difference between the AFP mRNA-positive and -negative groups in terms of protein induced by vitamin K antigen II (PIVKA-II) (p<0.05), but not in the other clinicopathologic parameters analyzed. Among 53 patients who underwent pre-operative TACE, 5 patients were AFP mRNA-positive, and pre-operative AFP mRNA was negative in 12 patients who showed complete TACE-related necrosis, although the statistical difference was not significant (p=0.20). Quantification of AFP mRNA revealed that AFP mRNA-positive patients who received pre-operative TACE had the worst overall survival after hepatectomy compared to the AFP mRNA-negative patients. Among the pre-operative TACE group, the 5-year overall survival rates were 60.0% for the AFP mRNA-positive group (n=5), and 88.8% for the AFP mRNA-negative group (n=48), respectively (p=0.02). Also, AFP mRNA-positive patients with a tumor size ≥5 cm showed similar results; the 5-year overall survival rates were 0% (n=2; each 0.4 and 1.25 years), and 83.3% (n=20), respectively (p=<0.01).

Discussion

One of the reasons for the high recurrence rate in HCC is postulated to be the potential hematogenous spread of cancer

cells pre- or intra-operatively, even if curative resection is performed. This possible phenomenon is probably due to the characteristics of HCC or the surgical manipulation during hepatectomy itself. Irrespective of the underlying etiology, it is important to control this hematogenous spread of cancer cells, and one of the purposes of pre-operative TACE is to prevent such spread and improve the outcome after curative resection.

In order to improve the survival rate after surgery for HCC, several researchers have tried pre-operative TACE; however, its clinical benefits are still controversial (Table IV) (9-29). Half of these studies including randomized controlled trials (RCTs) demonstrated effective results regarding pre-operative TACE while others did not or showed harmful results. Our results showed that pre-operative TACE prolonged the disease-free survival in patients with HCC tumors measuring 5 cm or more in diameter. In these previous studies, some authors supported our results, i.e., pre-operative TACE was effective in large or stage III-IV tumors (9-12). On the other hand, two RCTs showed the opposite results (20,22). However, the background of these patients differed from ours; both studies involved large tumor (≥10 cm) in hepatitis B carriers.

Subgroup analysis based on other clinicopathological factors, such as portal vein invasion, intrahepatic metastasis and TNM stage, which are considered important factors in the prognosis of HCC patients, showed that pre-operative TACE had no significant benefits to survival. Several studies have documented the poor response to TACE in patients with satellite lesions, intrahepatic recurrence or tumor thrombosis (12,13,25,26). The generally poor response of patients with portal vein invasion, intrahepatic metastasis or advanced HCC to pre-operative TACE and subsequently to surgery, may be explained by the aforementioned reasons.

On the other hand, our results suggest that pre-operative TACE is beneficial for patients with HCCs 5 cm or more in diameter. Of these patients, the mortality rate of AFP mRNA-positive patients was worse, even when they underwent pre-operative TACE. Although this finding may suggest hematological spread of cancer cells before surgery, the change in AFP mRNA levels should be analyzed before or after both pre-operative TACE and surgery, since it is doubtful whether pre-operative AFP mRNA was positive before TACE or became positive after TACE. Nonetheless, AFP mRNA may be a good prognostic marker of HCC.

The relationships between TACE-induced tumor necrosis, tumor spread and survival remain controversial (10-18,22-26). Our results showed that the 5-year overall and disease-free survival of patients with tumors showing a necrosis rate of 70% or higher was more favorable than the survival of patients with tumors showing less than 70% necrosis. In agreement with these results, the pre-operative AFP mRNA of all 12 patients who showed TACE-related complete necrosis was negative. Furthermore, the analysis of recurrence sites found that patients bearing tumors with a necrosis rate less than 70% were more likely to develop extrahepatic recurrence. Previous studies reported a higher incidence of extrahepatic metastasis in AFP mRNA-positive patients, either before or after TACE (32). These data indicate that complete necrosis induced by pre-operative TACE seems to inhibit extrahepatic metastasis and may be a suitable marker of favorable patient outcome.

Although the necrosis rate was determined through histopathological examination, some studies have evaluated the therapeutic response of TACE using modalities including dynamic CT, contrast-enhanced sonography, power Doppler sonography, dynamic MRI and angiography (33,34). However, we consider it insufficient to assess the effect of TACE pre-operatively. On the other hand, although the number of samples in this study was limited, the necrosis rate in 4 of the 5 (80%) AFP mRNA-positive patients who received pre-operative TACE was less than 70%. These findings suggest differences in survival between patients bearing tumors with a necrosis rate equal to or greater than 70 and patients bearing tumors with less than 70% necrosis. Although further examination is required, we can anticipate the efficacy of AFP mRNA in peripheral blood for patient survival after surgery following TACE.

In conclusion, pre-operative TACE may be beneficial for patients with HCC tumors measuring more than 5 cm in diameter. These patients should undergo TACE before curative resection to prolong disease-free survival. However, tumor necrosis equal to or greater than 70% is necessary for more favorable survival. Our results also showed that quantification of AFP mRNA in peripheral blood after TACE is potentially useful for the prediction of HCC recurrence.

Acknowledgements

We thank Yukari Sugita for measuring the AFP mRNA in peripheral blood. This study was supported by a Grant-in-Aid for Cancer Research from the Ministry of Culture and Science, and the Ministry of Health and Welfare of Japan.

References

1. Poon RT, Fan ST, Tsang FH and Wong J: Locoregional therapies for hepatocellular carcinoma: a critical review from the surgeon's perspective. Ann Surg 235: 466-486, 2002.
2. Witzigmann H, Geissler F, Benedix F, *et al*: Prospective evaluation of circulating hepatocytes by alpha-fetoprotein messenger RNA in patients with hepatocellular carcinoma. Surgery 131: 34-43, 2002.
3. Lemoine A, Le Bricon T, Salvucci M, *et al*: Prospective evaluation of circulating hepatocytes by alpha-fetoprotein mRNA in humans during liver surgery. Ann Surg 226: 43-50, 1997.
4. Kamiyama T, Takahashi M, Nakagawa T, *et al*: AFP mRNA detected in bone marrow by real-time quantitative RT-PCR analysis predicts survival and recurrence after curative hepatectomy for hepatocellular carcinoma. Ann Surg 244: 451-463, 2006.
5. Morimoto O, Nagano H, Miyamoto A, *et al*: Association between recurrence of hepatocellular carcinoma and alpha-fetoprotein messenger RNA levels in peripheral blood. Surg Today 35: 1033-1041, 2005.
6. Miyamoto A, Nagano H, Sakon M, *et al*: Clinical application of quantitative analysis for detection of hematogenous spread of hepatocellular carcinoma by real-time PCR. Int J Oncol 18: 527-532, 2001.
7. Marubashi S, Dono K, Sugita Y, *et al*: Alpha-fetoprotein mRNA detection in peripheral blood for prediction of hepatocellular carcinoma recurrence after liver transplantation. Transplant Proc 38: 3640-3642, 2006.
8. Marubashi S, Dono K, Nagano H, *et al*: Detection of AFP mRNA-expressing cells in the peripheral blood for prediction of HCC recurrence after living donor liver transplantation. Transpl Int 20: 576-582, 2007.

9. Peng BG, He Q, Li JP and Zhou F: Adjuvant transcatheter arterial chemoembolization improves efficacy of hepatectomy for patients with hepatocellular carcinoma and portal vein tumor thrombus. Am J Surg 198: 313-318, 2009.
10. Sugo H, Futagawa S, Beppu T, Fukasawa M and Kojima K: Role of pre-operative transcatheter arterial chemoembolization for resectable hepatocellular carcinoma: relation between postoperative course and the pattern of tumor recurrence. World J Surg 27: 1295-1299, 2003.
11. Zhong C, Guo RP, Li JQ, *et al*: A randomized controlled trial of hepatectomy with adjuvant transcatheter arterial chemoembolization versus hepatectomy alone for Stage III A hepatocellular carcinoma. J Cancer Res Clin Oncol 135: 1437-1445, 2009.
12. Lu CD, Peng SY, Jiang XC, Chiba Y and Tanigawa N: Pre-operative transcatheter arterial chemoembolization and prognosis of patients with hepatocellular carcinomas: retrospective analysis of 120 cases. World J Surg 23: 293-300, 1999.
13. Di Carlo V, Ferrari G, Castoldi R, *et al*: Pre-operative chemoembolization of hepatocellular carcinoma in cirrhotic patients. Hepatogastroenterology 45: 1950-1954, 1998.
14. Majno PE, Adam R, Bismuth H, *et al*: Influence of pre-operative transarterial lipiodol chemoembolization on resection and transplantation for hepatocellular carcinoma in patients with cirrhosis. Ann Surg 226: 688-703, 1997.
15. Harada T, Matsuo K, Inoue T, Tamesue S and Nakamura H: Is preoperative hepatic arterial chemoembolization safe and effective for hepatocellular carcinoma? Ann Surg 224: 4-9, 1996.
16. Gerunda GE, Neri D, Merenda R, *et al*: Role of transarterial chemoembolization before liver resection for hepatocarcinoma. Liver Transpl 6: 619-626, 2000.
17. Imaoka S, Sasaki Y, Shibata T, *et al*: A pre-operative chemoembolization therapy using lipiodol, cisplatin and gelatin sponge for hepatocellular carcinoma. Cancer Chemother Pharmacol 23: S126-S128, 1989.
18. Adachi E, Matsumata T, Nishizaki T, Hashimoto H, Tsuneyoshi M and Sugimachi K: Effects of pre-operative transcatheter hepatic arterial chemoembolization for hepatocellular carcinoma. The relationship between postoperative course and tumor necrosis. Cancer 72: 3593-3598, 1993.
19. Zhang Z, Liu Q, He J, Yang J, Yang G and Wu M: The effect of pre-operative transcatheter hepatic arterial chemoembolization on disease-free survival after hepatectomy for hepatocellular carcinoma. Cancer 89: 2606-2612, 2000.
20. Wu CC, Ho YZ, Ho WL, Wu TC, Liu TJ and P'Eng FK: Pre-operative transcatheter arterial chemoembolization for resectable large hepatocellular carcinoma: a reappraisal. Br J Surg 82: 122-126, 1995.
21. Yamasaki S, Hasegawa H, Kinoshita H, *et al*: A prospective randomized trial of the preventive effect of pre-operative transcatheter arterial embolization against recurrence of hepatocellular carcinoma. Jpn J Cancer Res 87: 206-211, 1996.
22. Zhou WP, Lai EC, Li AJ, *et al*: A prospective, randomized, controlled trial of pre-operative transarterial chemoembolization for resectable large hepatocellular carcinoma. Ann Surg 249: 195-202, 2009.
23. Monden M, Okamura J, Sakon M, *et al*: Significance of transcatheter chemoembolization combined with surgical resection for hepatocellular carcinomas. Cancer Chemother Pharmacol 23: S90-S95, 1989.
24. Paye F, Jagot P, Vilgrain V, Farges O, Borie D and Belghiti J: Pre-operative chemoembolization of hepatocellular carcinoma: a comparative study. Arch Surg 133: 767-772, 1998.
25. Sasaki A, Iwashita Y, Shibata K, Ohta M, Kitano S and Mori M: Pre-operative transcatheter arterial chemoembolization reduces long-term survival rate after hepatic resection for resectable hepatocellular carcinoma. Eur J Surg Oncol 32: 773-779, 2006.
26. Choi GH, Kim DH, Kang CM, *et al*: Is pre-operative transarterial chemoembolization needed for a resectable hepatocellular carcinoma? World J Surg 31: 2370-2377, 2007.
27. Nagasue N, Galizia G, Kohno H, *et al*: Adverse effects of pre-operative hepatic artery chemoembolization for resectable hepatocellular carcinoma: a retrospective comparison of 138 liver resections. Surgery 106: 81-86, 1989.
28. Uchida M, Kohno H, Kubota H, *et al*: Role of pre-operative transcatheter arterial oily chemoembolization for resectable hepatocellular carcinoma. World J Surg 20: 326-331, 1996.
29. Lee KT, Lu YW, Wang SN, *et al*: The effect of pre-operative transarterial chemoembolization of resectable hepatocellular carcinoma on clinical and economic outcomes. J Surg Oncol 99: 343-350, 2009.
30. Seldinger SI: Catheter replacement of the needle in percutaneous arteriography; a new technique. Acta Radiol 39: 368-376, 1953.
31. Dindo D, Demartines N and Clavien PA: Classification of surgical complications: a new proposal with evaluation in a cohort of 6336 patients and results of a survey. Ann Surg 240: 205-213, 2004.
32. Gross-Goupil M, Saffroy R, Azoulay D, *et al*: Real-time quantification of AFP mRNA to assess hematogenous dissemination after transarterial chemoembolization of hepatocellular carcinoma. Ann Surg 238: 241-248, 2003.
33. Jang MK, Lee HC, Kim IS, *et al*: Role of additional angiography and chemoembolization in patients with hepatocellular carcinoma who achieved complete necrosis following transarterial chemoembolization. J Gastroenterol Hepatol 19: 1074-1080, 2004.
34. Herber S, Biesterfeld S, Franz U, *et al*: Correlation of multislice CT and histomorphology in HCC following TACE: predictors of outcome. Cardiovasc Intervent Radiol 31: 768-777, 2008.

Hepatology Research

Hepatology Research 2010; 40: 793–798 doi: 10.1111/j.1872-034X.2010.00689.x

Original Article

Isolated metastasis to the gallbladder from hepatocellular carcinoma

Masahiro Murakami,[1] Shogo Kobayashi,[1] Shigeru Marubashi,[1] Hidetoshi Eguchi,[1] Yutaka Takeda,[1] Masahiro Tanemura,[1] Hiroshi Wada,[1] Koji Umeshita,[2] Wakasa Kennichi,[3] Yuichiro Doki,[1] Masaki Mori[1]* and Hiroaki Nagano[1]

[1]*Department of Surgery and* [2]*Department of Health Science, Graduate School of Medicine, Osaka University, and* [3]*Department of Pathology, Osaka City University Hospital, Osaka, Japan*

Aim: Metastasis to gallbladder (GB) from hepatocellular carcinoma (HCC) is rare, and it is difficult to determine indications for surgery. We report eight cases of synchronous isolated GB metastasis, and analyze their features retrospectively.

Methods: Among 439 HCC patients who underwent hepatectomy from 1998 to 2008 at our institution, 393 (89.5%) underwent concurrent cholecystectomy.

Results: Among them, eight (1.8%) had GB metastasis without other distant metastases. None of these cases showed evidence of direct invasion. All cases had advanced portal vein thrombus (PVTT) and their main tumor located near the GB bed. Five cases had apparent tumor mass in the GB wall, and the other three cases had only tumor thrombus in the GB veins. Six cases were treated postoperatively with local infusion therapy with interferon, and three of them showed long-term survival.

Conclusion: Our eight cases of GB metastasis from HCC were closely related to PVTT. Surgical resection and multimodal treatment would be necessary for long-term survival in cases with isolated GB metastasis.

Key words: hepatocellular carcinoma, gallbladder metastasis, portal vein tumor thrombus.

INTRODUCTION

HEPATOCELLULAR CARCINOMA (HCC) commonly shows intrahepatic spread, compared to extrahepatic metastasis, even in advanced-stage tumors. The majority of extrahepatic metastasis lesions are found in the lung, bone, and distant lymph nodes.[1,2] The gallbladder (GB) is a unique organ with respect to metastasis of HCC because it is anatomically adjacent to the liver, and advanced HCC commonly invades the GB directly.[3–6] On the other hand, an isolated metastasis to the GB from HCC is rare, with only three cases reported (two synchronous found unexpectedly and one metachronous); all were resected.[7–9]

We encountered eight patients, each with an isolated GB metastasis from HCC, who also presented with portal vein tumor thrombus (PVTT). Here, we report these cases and discuss the pattern of spread to the GB and treatment.

Correspondence: Dr Hiroaki Nagano, Department of Surgery, Graduate School of Medicine, Osaka University, 2-2 Yamadaoka E-2, Suita, 565-0871, Osaka, Japan. Email: hnagano@gesurg.med.osaka-u.ac.jp

Received 1 March 2010; revision 20 April 2010; accepted 3 May 2010.

PATIENTS AND METHODS

WE ENCOUNTERED EIGHT patients with synchronous GB metastasis among 439 patients who underwent hepatectomy for HCC between 1998 and 2008. Of this group, 57 patients (13.0%) had PVTT in the right or left branch of the portal vein or in the main trunk, 85 patients (19.4%) were in stage III, and 112 (25.5%) were in stage IV HCC.

Our routine preoperative examination for these patients included computed tomography (CT) scanning and magnetic resonance imaging (MRI), while hepatic angiography and arterial portography was carried out if indicated. In the patients with PVTT, we performed chest and brain CT, and bone scintigraphy to rule out distant metastasis. After these routine preoperative examinations, partial or functional anatomical liver resection was performed according to the preoperative or

intraoperative findings.[10,11] Briefly, the selected surgery was based on the tumor stage and liver function tests, such as Child–Pugh grade (A or B) and the value of the plasma retention rate of indocyanine green at 15 min (ICG-R15). Cholecystectomy was generally performed before hepatectomy as a standard technique in the cases of hemihepatectomy or to prevent cholecystitis following transarterial chemoembolization (TACE) for recurrent HCCs, if necessary. We resected the GBs of 393 patients and examined samples histopathologically. Briefly, all layers of the GB were dissected along the long axis and formalin-fixed when no macroscopically apparent tumor mass was found on the mucosa or in the wall. The specimens were examined microscopically after hematoxylin and eosin staining.

Herein we present a retrospective analysis of eight patients with HCC, in whom GB metastases were found incidentally following routine chlecyctectomy.

RESULTS

Patient characteristics

TABLE 1 SUMMARIZES the clinical characteristics of the patients studied. The mean age of the patient cohort was 56.8 years (range, 32–79 years), and all were men. Two cases had hepatitis B virus (HBV), two had hepatitis C virus, two had alcoholic hepatitis (Alc), and two had both HBV and Alc. Six cases were classified as Child–Pugh grade A and two as grade B.

Preoperative imaging diagnosis

All the current GB metastases were identified only by histopathological examination after surgical resection. That is, preoperative imaging showed no evidence of direct invasion or metastasis of the GB from the intrahepatic main tumor. In some cases, imaging showed wall thickening in the GB (Fig. 1, cases 3 and 7) or gallstones (GS) (case 1). In addition, one case showed dilation of the GB vein on CT (case 4).

Features of the main tumor

The location of the main tumor was at or near the center of the GB bed (seven of eight cases had tumor in segment (S) 4 or 5). The maximum tumor size was 5–15 cm. One case had a single tumor, thes others had multiple. The intraoperative findings included no direct invasion or metastasis to the GB and no distant metastases.

Treatment

Three patients underwent TACE before surgical resection (cases 5, 7, and 8). Six patients received postoperative

Table 1 Clinical characteristics and treatment

Case	Age (years)/ Sex (Male)	Background	Child-Pugh grade	Pre-operative image of GB	HCC			Pre-treatment	Hepatectomy	R	Post-therapy
					Location	Size (cm)	Number				
1	53/M	HBV Alc	A	GS	S7/8	14	Mt	None	Right	0	FAIT
2	61/M	HCV	A	np	S5/8	9.5	Mt	None	E-Right	0	FAIT
3	79/M	Alc	A	Wall thickness	S2/3/4	13	Mt	None	E-Left	2	FAIT
4	47/M	HBV	A	GB dilation	S4	6.5	Mt	None	Left	0	FAIT
5	47/M	HBV	A	np	S2/3/4	13	Mt	TACE	E-Left	2	FAIT
6	32/M	HBV Alc	A	np	S5/6/7/8	15	Mt	None	E-Right	2	FAIT
7	74/M	HCV	B	Wall thickness	S5/6	5	St	TACE	Right	0	none
8	66/M	Alc	B	np	S5/8	3.5	Mt	TACE	Anterior	2	none

Alc, alcoholic hepatitis; E-, extended; FAIT, intraarterial infusion of 5-FU and subcutaneous interferon-alpha injection therapy; GS, gall stone; HBV, hepatitis B virus; HCV, hepatitis C virus; Mt, multiple tumors; np, no problem; post-therapy, postoperative therapy including adjuvant setting; St, single tumor; TACE, *trans*-arterial chemoembolization.

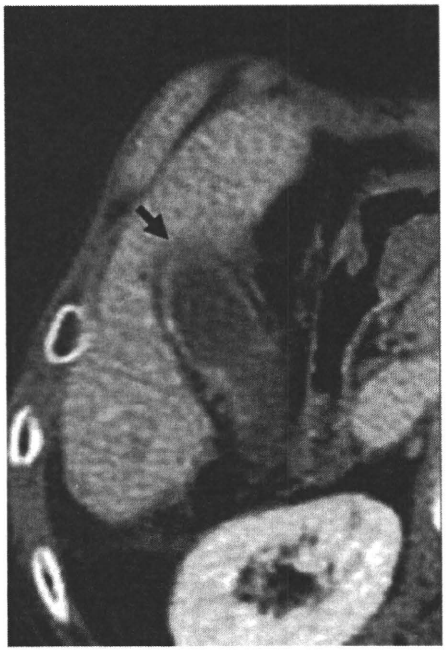

Figure 1 Computed tomography scan showing gallbladder wall thickness.

chemotherapy with IFN (IFN/5-FU) as an adjuvant-setting or multimodal approach (cases 1–6).

Table 2 details the histopathological characteristics and postoperative outcomes of all patients.

Histopathological characteristics

All patients had PVTT in the right or left branch of the portal vein or in the main trunk, but none had lymph node metastasis. One patient showed invasion of the right hepatic vein (case 2) and another showed bile duct invasion in the right hepatic duct (case 8). Postoperative histopathological examination revealed poorly differentiated HCC of the main tumor in seven cases. All cases had tumor thrombus in the GB blood or lymph vessels and three cases showed tumor thrombus in the GB vein without apparent tumor mass in the mucosa or wall (GBTT) only (cases 1–3, Fig. 2).

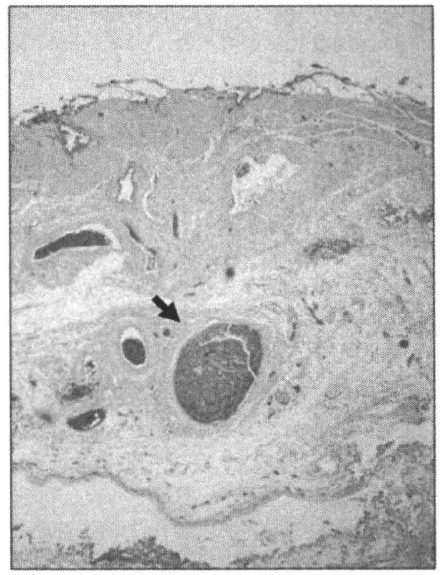

Figure 2 Histopathological staining showing representative tumor thrombus in GB veins (hematoxylin and eosin, ×100).

Adjuvant therapy and postoperative outcome

Three patients exhibited a good response to IFN/5-FU therapy and long-term survival postoperatively (cases 1,

Table 2 Histopathological characteristics and outcome

Case	PVTT	*n*	Other invasion site	Histological type	Edmondson grade	Distribution of meta	DFS (day)	Recurrence site	OS (day)	Prognosis
1	Main	0	None	Poor	III	GBTT	597	Lung	1914	Alive
2	Main	0	RHV	Poor	III	GBTT	121	None	121	Alive
3	Main	0	None	Mod	II	GBTT	0	Liver/lung	185	Died
4	Lt	0	None	Poor	III	mp	1643	Lung	1643	Died
5	Main	0	None	Poor	III > IV	mp	0	Other	271	Died
6	Main	0	None	Poor	III	mp	0	Liver	89	Died
7	Main	0	None	Poor	III	sm	110	Liver	145	Died
8	Main	0	RHD	Poor	III	m-mp	0	Liver/LN	175	Died

DFS, disease-free survival; GBTT; gallbladder vein tumor thrombus; Lt, left; m-mp, mucosal layer-muscle layer; LN, lymph node metastasis; mod, moderate; OS, overall survival; pm, the organ developed metastasis after surgery; PVTT, portal vein invasion; RHD, right hepatic duct; RHV, right hepatic vein; sm, submucosal layer.

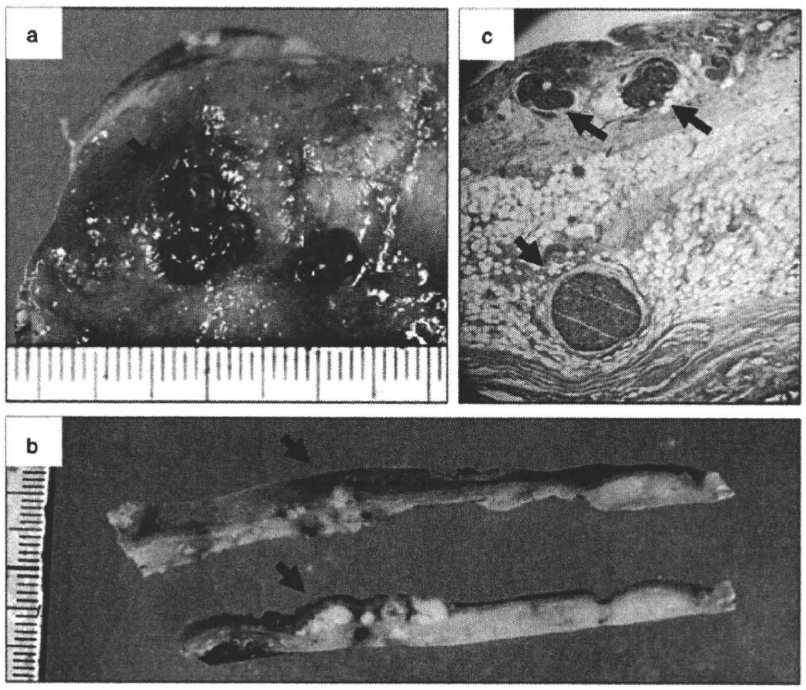

Figure 3 A typical case of gallbladder metastasis (case 8). The tissue showed (a,b) some small protruding lesion on the mucosa and white nodes in the GB wall on macroscopic examination, while (c) histopathological examination revealed poorly differentiated heptaocellular carcinoma cells in the lamina propria and muscle layer of the gallbladder, and invasion into the submucosal vessels (hematoxylin and eosin, ×100).

2, and 4), although the same treatment was ineffective for another three cases (Cases 3, 5, and 6). Although case 4 subsequently died of liver failure without HCC recurrence, the other deaths among IFN/5-FU-treated patients after surgical resection were from recurrent cancer, located mostly in liver or lung. Two patients could not have any treatment due to liver failure (cases 7 and 8). Two of the three cases with GBTT only remain alive.

Below we present two cases as representative of GBTT only and metastasis to GB, respectively.

Case 1

A 53-year-old man was admitted to our hospital for advanced HCC. CT and MRI scans showed tumor located mainly in S7/8, with PVTT and GS. We performed right hepatectomy, tumor thrombectomy, and cholecystectomy. Although the macroscopic examination showed no tumorous lesion in the mucosa or wall of the GB, histopathological examination showed GBTT only (Fig. 2). The patient received IFN/5-FU therapy postoperatively, followed by pneumectomy for metachronous lung metastasis and chemotherapy with IFN. The patient is still alive with no recurrence.

Case 8

A 74-year-old man had advanced HCC with tumor located mainly in the posterior segment as well as PVTT. Imaging showed an edematous and thick GB wall that was not adjacent to the main tumor. We performed an extended posterior segmentectomy, tumor thrombectomy, and cholecystectomy. Macroscopically, the tissue showed some small protruding lesions on the mucosa and white nodes in the GB wall (Fig. 3a). Histopathological examination revealed poorly-differentiated HCC, as seen in the main tumor, in the lamina propria and muscle layer of the GB, as well as invasion of the submucosal vessels (Fig. 3b). The diagnosis was therefore GB metastasis from HCC. The patient could not have any treatment and subsequently died of liver failure.

DISCUSSION

GB METASTASIS FROM HCC is a rare clinical occurrence. Autopsy studies report the frequency of GB metastasis as approximately 5%,[13–17] with the clinical features of GB metastasis mostly described as advanced stage with multiple metastasis sites.

In contrast, a resected isolated GB metastasis is rarely encountered. Here, we considered three surgically resected cases reported previously (Table 3).[7–9] A comparison of these and our cases revealed that 10 of 11 cases had PVTT. HCC with PVTT is not usually an indication for surgical resection alone and requires instead a

Table 3 Summary of reported cases of metastatic gallbladder tumors from HCC

Case	Period	HCC			Treatment	Outcome	Reference
		Location	PVTT	Histology			
48/M	Synchronous	S4/5	Yes	Mod	Hepatectomy + Cholecystectomy	Not described	Nishida *et al.*[5]
49/M	Metachronous	S5/6/7/8	Yes	Mod	IFN + chemo Tx† →Cholecystectomy	13 months alive	Terashima *et al.*[6]
73/M	Synchronous	S4	None	Mod	Hepatectomy + Cholecystectomy	32 months alive	Maruo *et al.*[7]

†chemo Tx: Methotrexate (MTX) + cisplatin (CDDP) + 5FU + Leucovorin (LV). HCC, hepatocellular carcinoma; IFN, interferon; IFN, interferon; mod, moderate; PVTT, portal vein tumor thrombus.

multimodal approach.[18] Recently, we reported excellent clinical outcomes with IFN/5-FU combination therapy for highly advanced HCC with PVTT.[19–22] We propose that some of the cases of advanced HCC that were treated as inoperable already had undetected GB metastasis. This background allowed us to identify the eight cases of GB metastasis described in this report. Analysis of patients with HCC and PVTT showed that approximately 14.0% of patients with HCC and PVTT had an isolated GB metastasis.

Based on the current and previously published data, a link between PVTT and GB metastasis is feasible, suggesting direct metastasis from HCC to the GB. In support of this notion, most cases had PVTT and the main tumors were located at or near the GB bed (S4 and S5). In terms of primary GB malignancy, the GB vein is thought to fully drain into the portal vein system and thus is a possible metastatic route from the liver. This suggests a possible interaction between the portal and GB veins.[23–25] In addition, cases 1–3 showed micrometastases and case 4 had GB vein dilatation on CT. These data support our hypothesis that HCC cells could access the GB vein via the portal vein adversely because of portal hypertension associated with PVTT or liver cirrhosis, and then infiltrate outside the vascular wall to develop tumor in the GB, especially in advanced HCC cases with PVTT. The GB vein dilatation would be caused by tumor thrombi in the GB vein.

Based on this hematogenous route of GB spread, it would be difficult to define such "metastasis" according to classical histopathological criteria; a better definition could be "local extension". In fact, we treated six of eight patients with incidental GB metastasis with surgical resection and IFN/5-FU therapy as local infusion therapy. In four of these cases, liver recurrences were well controlled and three are still surviving disease-free (cases 1, 2, and 4). Based on our experience, an isolated GB metastasis could therefore be treated by intensive local control with surgical resection and local infusion therapy (IFN/5-FU therapy or TACE) under the controllable condition of liver recurrence.

Finally, the indication of surgical resection for isolated GB metastasis is summarized as follows. Since most GB metastasis cases had PVTT, a suspicion of GB metastasis on preoperative routine imaging should be treated as HCC with PVTT; surgical resection including the afferent portal vein and GB is recommended, followed by IFN/5-FU therapy. On the other hand, cases of advanced HCC with PVTT showing a normal GB on preoperative imaging should be monitored carefully during surgery for micrometastasis in the GB; we routinely perform concurrent cholecystectomy prior to resection of HCC with PVTT.[26] Such cases then require IFN/5-FU therapy postoperatively to prevent HCC recurrence in remnant liver, and careful histopathological examination to detect macro- or micro-metastasis in the GB. In the case of early-stage HCC indicated for partial hepatectomy, cholecystectomy is not always necessary due to the low risk of GB metastasis.

In conclusion, GB metastasis could be caused by PVTT via local hematological spread and should be treated as local extension. Surgical resection and multimodal treatment, such as IFN/5-FU therapy, could contribute to long-term survival in cases with isolated GB metastasis.

REFERENCES

1 Kanda M, Tateishi R, Yoshida H *et al.* Extrahepatic metastasis of hepatocellular carcinoma: incidence and risk factors. *Liver Int* 2008; **28**: 1256–63.
2 Hong SS, Kim TK, Sung KB *et al.* Extrahepatic spread of hepatocellular carcinoma: a pictorial review. *Eur Radiol* 2003; **13**: 874–82.
3 Yuki K, Hirohashi S, Sakamoto M, Kanai T, Shimosato Y. Growth and spread of hepatocellular carcinoma. A review of 240 consecutive autopsy cases. *Cancer* 1990; **66**: 2174–9.
4 Terasaki S, Nakanuma Y, Terada T, Unoura M. Metastasis of hepatocellular carcinoma to the gallbladder presenting

massive intraluminal growth: report of an autopsy case. *J Clin Gastroenterol* 1990; **12**: 714–5.
5 Nakashima T, Okuda K, Kojiro M *et al.* Pathology of hepatocellular carcinoma in Japan. 232 Consecutive cases autopsied in ten years. *Cancer* 1983; **51**: 863–77.
6 Nakashima O, Sugihara S, Eguchi A, Taguchi J, Watanabe J, Kojiro M. Pathomorphologic study of pale bodies in hepatocellular carcinoma. *Acta Pathol Jpn* 1992; **42**: 414–8.
7 Terashima T, Yamashita T, Arai K *et al.* A case of metastatic gallbladder tumor of the hepatocellular carcinoma (in Japanese with English abstract). *Kanzo* 2007; **48**: 363–9.
8 Nishida J, Tanaka M, Suto K *et al.* A case of metastatic gall bladder tumor derived from hepatocellular carcinoma (in Japanese with English abstract). *Nippon Shokakibyo Gakkai Zasshi (Jpn J Gastroenterol)* 1997; **94**: 857–60.
9 Maruo H, Watahiki Y, Ohsaku M, Kosaka A, Mori I. A case of hepatocellular carcinoma with metastasis to the gall bladder and the omentum. *Gastroent Surgery* 1994; **17**: 1379–83.
10 Sakon M, Nagano H, Nakamori S *et al.* Intrahepatic recurrences of hepatocellular carcinoma after hepatectomy: analysis based on tumor hemodynamics. *Arch Surg* 2002; **137**: 94–9.
11 Sakon M, Nagano H, Shimizu J *et al.* Hepatic resection of hepatocellular carcinomas based on tumor hemodynamics. *J Surg Oncol* 2000; **73**: 179–81.
12 Wittekind C, Compton CC, Greene FL, Sobin LH. TNM residual tumor classification revisited. *Cancer* 2002; **94**: 2511–6.
13 Ueno N, Kanamaru T, Kawaguchi K *et al.* A hepatocellular carcinoma with lymph node metastasis and invasion into the gallbladder: preoperative difficulty ruling out a gallbladder carcinoma. *Oncol Rep* 2001; **8**: 331–5.
14 Tamura S, Kihara Y, Kakitsubata Y *et al.* Hepatocellular carcinoma invading the gallbladder: CT, arteriography and MRI findings. *Clin Imaging* 1993; **17**: 109–11.
15 Miura F, Asano T, Nakagori T *et al.* A case of hepatocellular carcionoma invading the gall bladder which was difficult to make differential diagnosis from gall bladder carcinoma. *Liver Cancer* 1996; **2**: 157–61.
16 Kumagaya Y. A histological study of hepatocellular carcinoma obstruction of the common bile duct by intraductal growth (in Japanese with English abstract). *Kanzo* 1979; **20**: 157–63.
17 Chiba M, Saito A, Hayashi N. Hepatocellular carcinoma invades the gallbladder via vessels. *J Hepatol* 2002; **37**: 411.
18 Minagawa M, Makuuchi M. Treatment of hepatocellular carcinoma accompanied by portal vein tumor thrombus. *World J Gastroenterol* 2006; **12**: 7561–7.
19 Sakon M, Nagano H, Dono K *et al.* Combined intraarterial 5-fluorouracil and subcutaneous interferon-alpha therapy for advanced hepatocellular carcinoma with tumor thrombi in the major portal branches. *Cancer* 2002; **94**: 435–42.
20 Ota H, Nagano H, Sakon M *et al.* Treatment of hepatocellular carcinoma with major portal vein thrombosis by combined therapy with subcutaneous interferon-alpha and intra-arterial 5-fluorouracil; role of type 1 interferon receptor expression. *Br J Cancer* 2005; **93**: 557–64.
21 Nagano H, Sakon M, Eguchi H *et al.* Hepatic resection followed by IFN-alpha and 5-FU for advanced hepatocellular carcinoma with tumor thrombus in the major portal branch. *Hepatogastroenterology* 2007; **54**: 172–9.
22 Nagano H, Miyamoto A, Wada H *et al.* Interferon-alpha and 5-fluorouracil combination therapy after palliative hepatic resection in patients with advanced hepatocellular carcinoma, portal venous tumor thrombus in the major trunk, and multiple nodules. *Cancer* 2007; **110**: 2493–501.
23 Yoshimitsu K, Honda H, Kaneko K *et al.* Anatomy and clinical importance of cholecystic venous drainage: helical CT observations during injection of contrast medium into the cholecystic artery. *AJR Am J Roentgenol* 1997; **169**: 505–10.
24 Sugita M, Ryu M, Satake M *et al.* Intrahepatic inflow areas of the drainage vein of the gallbladder: analysis by angio-CT. *Surgery* 2000; **128**: 417–21.
25 Kumaoka H, Kikuyama M, Kitanaka H *et al.* Cystic vein: as a perfusion vein of hepatic portion-angiographical study (in Japanese with English abstract). *Nippon Shokakibyo Gakkai Zasshi (Jpn J Gastroenterol)* 1998; **95**: 419–23.
26 Inoue Y, Hasegawa K, Ishizawa T *et al.* Is there any difference in survival according to the portal tumor thrombectomy method in patients with hepatocellular carcinoma? *Surgery* 2009; **145**: 9–19.

Hepatocellular Carcinoma: Hepatocyte-selective Enhancement at Gadoxetic Acid–enhanced MR Imaging—Correlation with Expression of Sinusoidal and Canalicular Transporters and Bile Accumulation[1]

Takahiro Tsuboyama, MD
Hiromitsu Onishi, MD, PhD
Tonsok Kim, MD, PhD
Hirofumi Akita, MD
Masatoshi Hori, MD, PhD
Mitsuaki Tatsumi, MD, PhD
Atsushi Nakamoto, MD
Hiroaki Nagano, MD, PhD
Nariaki Matsuura, MD, PhD
Kenichi Wakasa, MD, PhD
Kaname Tomoda, MD, PhD

Purpose: To investigate the mechanism of enhancement of hepatocellular carcinoma (HCC) on gadoxetic acid–enhanced hepatobiliary phase magnetic resonance (MR) images and to characterize HCC thus enhanced.

Materials and Methods: This retrospective study was approved by the institutional review board, and patient informed consent for research use of the resected specimen was obtained. MR images in 25 patients (20 men, five women; mean age, 68 years; range, 49–82 years) with 27 resected hypervascular HCCs (one well, 13 moderately, 13 poorly differentiated) that demonstrated hepatocyte-selective enhancement on gadoxetic acid–enhanced MR images, were quantitatively studied, and findings were correlated with results of immunohistochemical staining for a sinusoidal transporter, organic anion transporting polypeptide (OATP) 1B1 (OATP1B1) and/or OATP1B3 (OATP1B1 and/or -1B3), and a canalicular transporter, multidrug resistance–associated protein 2 (MRP2), and also with bile accumulation in tumors. Statistical analysis was performed with the Student *t* test and Scheffé post hoc test.

Results: Combined with positive OATP1B1 and/or -1B3 expression (O+), two patterns of MRP2 expression contributed to high enhancement: decreased expression (M−, $n = 3$) and increased expression at the luminal membrane of pseudoglands (M+[P], $n = 3$). Nodules without OATP1B1 and/or -1B3 expression (O−, $n = 13$) and nodules with O+ associated with increased MRP2 expression only at the canaliculi (M+[C], $n = 8$) induced significantly lower enhancement than those with the two expression patterns described before (O+/M− group vs O− group, $P = .002$; O+/M− group vs O+/M+[C] group, $P = .047$; O+/M+[P] group vs O− group, $P < .001$; O+/M+[P] group vs O+/M+[C] group, $P < .001$). Nodules with bile pigment ($n = 12$) showed significantly higher enhancement ($P = .004$); all five nodules (one well differentiated HCC, four moderately differentiated HCCs), which were enhanced more than adjacent liver parenchyma, contained bile pigment.

Conclusion: High hepatocyte-selective enhancement is induced by expression patterns of transporters, which may result in accumulation of gadoxetic acid in cytoplasm of tumor cells or in lumina of pseudoglands. An HCC with gadoxetic acid enhancement is characterized by bile accumulation in tumors.

Supplemental material: *http://radiology.rsna.org/lookup/suppl/doi:10.1148/radiol.10091557/-/DC1*

[1] From the Departments of Radiology (T.T., H.O., T.K., M.H., M.T., A.N., K.T.) and Surgery (H.A., H.N.), Osaka University Graduate School of Medicine, 2-2 Yamadaoka, Suita, Osaka 565-0871, Japan; Department of Molecular Pathology, Osaka University Graduate School of Medicine and Health Science, Osaka, Japan (N.M.); and Department of Pathology, Osaka City University Hospital, Osaka, Japan (K.W.). Received August 20, 2009; revision requested October 6; final revision received November 12; accepted December 16; final version accepted January 11, 2010. **Address correspondence to** T.T. (e-mail: *t-tsuboyama@radiol.med.osaka-u.ac.jp*).

Gadoxetic acid is a newly developed liver-specific contrast agent for magnetic resonance (MR) imaging (1). This agent is characterized by combined good extracellular and hepatocyte-selective properties (2). Approximately 50% of the administered dose is taken up by hepatocytes and excreted into bile, and this rate is much higher than the hepatic uptake of another liver-specific contrast agent, gadobenate dimeglumine (3). As a result of the hepatic uptake, maximal enhancement of normal liver parenchyma is obtained in the hepatobiliary phase, about 20 minutes after injection of gadoxetic acid (4), which thus allows for improved detection of focal liver lesions that lack functioning hepatocytes (2,5–7).

Positive enhancement at gadoxetic acid–enhanced hepatobiliary phase imaging occurs not only in normal liver parenchyma but also in focal liver lesions of hepatocellular origin, such as focal nodular hyperplasia (8,9). Some investigators have reported that positive hepatocyte-selective enhancement may also be observed in some patients with hepatocellular carcinoma (HCC) (7,8,10–12). This seemingly paradoxical enhancement of HCC was limited to well-differentiated HCC in some studies (8,11), whereas it was also observed in moderately or poorly differentiated HCC in other studies (7,10,12). However, little is known about the mechanism of this enhancement of HCC or about the characteristics of HCC thus enhanced.

It has been suggested that organic anion transporting polypeptides (OATPs), expressed at the basolateral membrane of hepatocytes, mediate the uptake of gadoxetic acid (13) and that multidrug resistance-associated protein 2 (MRP2), expressed in the canalicular membrane, mediates the secretion from hepatocytes (14). Of the OATP family, rat Oatp1a1 was demonstrated to be a carrier of gadoxetic acid, whereas human OATP1A2 was not involved in its uptake (15). This finding was followed by cloning of the most dominant OATPs in human liver, OATP1B1 and OATP1B3 (16,17), which are now considered promising candidates as potential transporters of gadoxetic acid in human liver.

Some investigators (10,18–22) have reported that HCC tumor cells expressed the hepatocellular transporters, including OATP1B1 and/or OATP1B3 (hereafter, OATP1B1 and/or -1B3) and MRP2. We therefore hypothesized that the degree of expression of these transporters in tumor cells may affect the kinetics of gadoxetic acid in tumors.

The purpose of this study was to investigate the mechanism of enhancement of HCC on gadoxetic acid–enhanced hepatobiliary phase MR images and to characterize HCC thus enhanced.

Advances in Knowledge

- Expression of a sinusoidal transporter, organic anion transporting polypeptide 1B1 (OATP1B1) and/or OATP1B3 (OATP1B1 and/or -1B3), is essential but not sufficient for high hepatocyte-selective enhancement of hepatocellular carcinoma (HCC) on gadoxetic acid–enhanced MR images, because all nodules with high enhancement showed positive expression of OATP1B1 and/or -1B3, whereas 64% of nodules with positive OATP1B1 and/or -1B3 expression demonstrated low enhancement.
- Combined with OATP1B1 and/or -1B3 expression, two expression patterns of a canalicular transporter, multidrug resistance–associated protein 2, contributed to high enhancement, a decreased expression and an increased expression at the luminal membrane of pseudoglands.
- HCC with high hepatocyte-selective enhancement is characterized by bile accumulation in tumors.

Implication for Patient Care

- HCC with bile accumulation should be included in the differential diagnosis for tumors with positive enhancement on gadoxetic acid–enhanced hepatobiliary phase MR images.

Materials and Methods

Patients

Institutional review board approval for this retrospective study was obtained from Osaka University Hospital (Osaka, Japan), and written informed consent for research use of the resected specimen was obtained from all patients. The surgery, pathology, and radiology records of patients with HCC who underwent surgery at our institution between April 1, 2008, and June 30, 2009, were reviewed. Inclusion criteria were preoperative gadoxetic acid–enhanced MR examination and presence of histopathologically proved nodular HCC at surgery. Forty-eight patients with 50 HCCs that were histopathologically proved by surgical resection were identified; 42 of these patients had undergone preoperative gadoxetic acid–enhanced MR examination within 2 months of the surgical procedure. Exclusion criteria included preoperative treatment, such as transcatheter arterial chemoembolization, and the presence of abnormal signal intensity (SI) in liver parenchyma adjacent to the tumor on MR images, because the correlation

Published online
10.1148/radiol.10091557

Radiology 2010; 255:824–833

Abbreviations:
HBV = hepatitis B virus
HCC = hepatocellular carcinoma
HCV = hepatitis C virus
MRP = multidrug resistance–associated protein
OATP = organic anion transporting polypeptide
ROI = region of interest
SI = signal intensity

Author contributions:
Guarantors of integrity of entire study, T.T., T.K.; study concepts/study design or data acquisition or data analysis/interpretation, all authors; manuscript drafting or manuscript revision for important intellectual content, all authors; approval of final version of submitted manuscript, all authors; literature research, T.T., H.O., M.H.; clinical studies, T.T., H.O., T.K., H.A., M.H., M.T., A.N., H.N., N.M., K.W.; statistical analysis, T.T.; and manuscript editing, T.T., H.O., T.K., K.T.

Authors stated no financial relationship to disclose.

Table 1

Summary of Relative Enhancement Ratios, Expression of Transporters, and Bile Pigment Findings

Patient No.*	Child-Pugh Class	Cause	Background Liver	Tumor Grade†	Tumor Size (mm)	Relative Enhancement Ratio	OATP1B1 and/or -1B3 Expression Score‡	MRP2 Expression Score ‡		Bile Pigment Score and Location#
								Canaliculus§	Pseudogland‖	
					Nodules with High Enhancement **					
1	A	HCV	Chronic hepatitis	M	25	1.48	1+	2+	2+	2+, pseudogland
2	A	HCV	Cirrhosis	W	14	1.39	2+	2+	2+	1+, pseudogland
3	B	HCV	Cirrhosis	M	28	1.13	2+	1+	NCS	2+, cytoplasm
4	A	Alcohol	Chronic hepatitis	M	27	1.13	2+	1+	1+	1+, cytoplasm
5	A	HCV	Chronic hepatitis	M	15	1.05	1+	2+	2+	1+, pseudogland
					Nodules with Low Enhancement††					
6	B	Unknown	Normal	M	29	0.86	0	NCS	2+	0
7	A	HCV	Cirrhosis	P	31	0.84	2+	2+	1+	1+, ND
8	A	HBV	Cirrhosis	P	30	0.84	1+	2+	1+	0
9	B	HCV	Cirrhosis	P	16	0.80	1+	2+	NCS	0
3	B	HCV	Cirrhosis	M	30	0.80	1+	2+	NCS	1+, cytoplasm
10	A	HCV	Cirrhosis	M	23	0.79	1+	1+	NCS	0
11	A	HBV	Chronic hepatitis	P	35	0.78	1+	2+	0	1+, pseudogland
12	A	HCV	Chronic hepatitis	M	15	0.78	1+	2+	NCS	0
13	B	HCV	Cirrhosis	P	13	0.78	0	2+	NCS	1+, ND
14	A	HCV	Cirrhosis	P	33	0.77	0	1+	1+	0
15	B	HBV	Cirrhosis	M	24	0.76	0	2+	1+	1+, cytoplasm
16	A	HBV	Cirrhosis	P	17	0.71	0	2+	NCS	0
17	A	HBV	Chronic hepatitis	P	30	0.70	2+	2+	0	0
18	A	HCV	Chronic hepatitis	M	10	0.69	0	2+	2+	1+, ND
19	A	HCV	Cirrhosis	P	17	0.69	0	2+	1+	0
20	A	HBV	Chronic hepatitis	M	37	0.66	0	2+	2+	0
21	A	Unknown	Normal	P	58	0.66	0	1+	0	0
22	A	HBV	Chronic hepatitis	M	18	0.65	1+	2+	NCS	0
23	A	HCV	Cirrhosis	P	10	0.64	0	1+	NCS	0
24	B	HCV	Cirrhosis	P	25	0.63	0	2+	0	1+, ND
19	A	HCV	Cirrhosis	P	21	0.52	0	1+	NCS	0
25	A	HBV	Chronic hepatitis	M	32	0.52	0	2+	0	0

* Patients are listed in descending order of values of relative enhancement ratios. Two nodules were assessed separately in patients 3 and 19.

† M = moderately differentiated HCC, W = well-differentiated HCC, P = poorly differentiated HCC.

‡ 0 = negative or minimal, 1+ = positive to the same or lesser extent than the liver parenchyma, 2+ = positive to a greater extent compared with liver parenchyma, NCS = no corresponding structure.

§ Expression at canalicular membrane of trabecular structure.

‖ Expression at luminal membrane of pseudoglandular structure.

The location of bile pigment was determined at microscopic examination. 0 = negative, 1+ = focal, 2+ = diffuse, ND = not detected.

** High enhancement = relative enhancement ratio greater than one.

†† Low enhancement = relative enhancement ratio less than one.

between the histopathologic and imaging findings and the comparison between the SI of the tumors and the SI of adjacent liver parenchyma were difficult. A total of 17 of 42 patients were excluded; 14 patients with 16 HCCs who underwent preoperative transcatheter arterial chemoembolization and three patients with three HCCs (two patients with recurrent tumor near the site of previous surgery and one patient with portal vein tumor thrombus) with abnormal SI in the adjacent liver parenchyma. Two HCCs included in this study consisted of two distinct nodules with different SI on contrast material–enhanced MR images (Table 1, patients 3 and 19), and each nodule was assessed separately. Finally, 25 patients with 27 HCC nodules were included in this study.

The patients ranged from 49 to 82 years of age (mean, 68 years). Twenty patients were men (mean age, 68 years; range, 49–82 years), and five were women (mean age, 70 years; range, 63–78 years). Thirteen patients had underlying liver cirrhosis and nine had chronic hepatitis, caused by hepatitis B virus (HBV) in eight patients and hepatitis C virus (HCV) in 14 patients. One patient had alcoholic chronic hepatitis, and two had a normal liver. In these patients, liver function was based on the

Table 2

Summary of the MR Examination

A: Liver Acquisition with Volume Acceleration Sequence	
Parameter	Value*
Repetition time (msec)	4.5/3.6
Echo time (msec)	2.2/1.7
Flip angle (degree)	12/12
Inversion time (msec)	7/5
Bandwidth (kHz)	62.5/83.8
Matrix	320 × 192/320 × 192
Field of view (mm)	340/340
Section thickness (mm)	4/4
Array spatial sensitivity-encoding technique factor	2/2
B: Gadoxetic Acid-enhanced Imaging Method	
Feature	Administration
Dose of gadoxetic acid	0.025 mmol per kilogram of body weight
Image delay	
For arterial phase	10 sec after triggering†
For portal venous phase	70 sec after injection
For equilibrium phase	180 sec after injection
For hepatobiliary phase	20 min after injection

Note.—All images were obtained in transverse plane.

* Data are values for 1.5-T system/3-T system.

† Triggering = the arrival of contrast material at the abdominal aorta.

Child-Pugh classification: In 19 patients, nodules were categorized as class A, and in six patients, nodules were categorized as class B. Tumors ranged in size from 10 to 58 mm (mean, 25 mm). All nodules were hypervascular tumors, showing hyperenhancement relative to the surrounding liver parenchyma in the arterial phase of the dynamic MR examination.

MR Examination

The MR examinations were performed with a 1.5-T MR system (Signa Excite HD; GE Healthcare, Milwaukee, Wis) in nine patients and with a 3-T system (Signa HDx; GE Healthcare) in the other 16 patients. An eight-channel phased-array coil system for the abdominopelvic region was used.

Images were obtained by using a breath-hold T1-weighted three-dimensional gradient-echo sequence (liver acquisition with volume acceleration, or LAVA) with fat suppression as follows: at imaging before administration of contrast agent, at dynamic triple-phase imaging after administration of gadoxetic acid (Primovist; Bayer-Schering Pharma AG, Berlin, Germany), and at hepatobiliary phase imaging. The parallel imaging technique (array spatial sensitivity encoding technique, or ASSET) also was used. The method for the MR examination is summarized in Table 2. Hepatobiliary phase imaging was performed 20 minutes after injection of contrast agent.

Histopathologic Analysis

Four-micrometer-thick tissue sections prepared from formalin-fixed paraffin-embedded blocks were stained with hematoxylin-eosin and were reviewed by two authors (K.W. and N.M., with 28 and 18 years of experience, respectively) who specialize in liver pathology. Histopathologic grading was determined according to criteria proposed previously (23–25). One nodule was classified as a well-differentiated HCC, 13 were classified as moderately differentiated HCCs, and 13 were classified as poorly differentiated HCCs. Pseudoglandular structures of various numbers and sizes were found in 17 nodules, and one of the tumors consisted of only pseudoglandular structures.

Immunohistochemical Staining

Immunohistochemical staining of tumors and the adjacent liver parenchyma was performed with a staining kit (Vectastain ABC Peroxidase Kit; Vector Laboratories, Burlingame, Calif) for OATP1B1 and/or -1B3 and MRP2 on 3.5-μm-thick, formalin-fixed, paraffin-embedded sections. Autoclave antigen retrieval in 10 mmol/L citrate buffer (pH 6.0) was performed, followed by endogenous peroxidase activity blocking with a 1% H_2O_2 solution in methanol. Serum blocking was performed by using 10% normal horse serum. The sections were incubated at 4°C overnight with primary monoclonal antibodies against OATP1B1 and/or -1B3 (clone mMDQ, 1:100) (Progen Biotechnik, Heidelberg, Germany) and MRP2 (clone M2III-6, 1:50) (Monosan, Uden, the Netherlands). Secondary biotinylated anti-mouse antibody (BA2000; Vector Laboratories) was used at a dilution of 1:100 at room temperature. The immunopositivity was visualized by means of 3,3′-diaminobenzidine. Sections were counterstained with hematoxylin.

Evaluation of MR Images

MR images were reviewed by two abdominal radiologists (H.O. and T.K., with 12 and 19 years of experience, respectively) who specialized in hepatic MR imaging. Quantitative analysis for tumor enhancement at hepatobiliary phase imaging was performed by the following method (26). First, the SI of tumors and the SI of the adjacent liver parenchyma were measured in regions of interest (ROIs) placed on precontrast and postcontrast hepatobiliary phase MR images. The two radiologists placed all ROIs at the section level of the largest tumor diameter devoid of necrosis in consensus. Tumor ROIs were determined by tracing the margin of the tumor, even though the SI was heterogeneous in each of the ROIs devoid of necrosis (mean ROI, 336 mm^2; range, 72–807 mm^2). ROIs on the adjacent liver parenchyma were determined by tracing the surrounding nontumorous region approximately within 20 mm from the tumor while avoiding vascular structures (mean ROI, 904 mm^2; range, 268–2544 mm^2).

Next, the relative intensity ratio was calculated on precontrast and postcontrast MR images, with the following formula: RIR = SI_{nod}/SI_{par}, where RIR is the relative intensity ratio, SI_{nod} is the SI of the nodule, and SI_{par} is the SI of the liver parenchyma. The enhancement of nodules compared with that of the liver parenchyma was defined as the relative enhancement ratio of nodules and was calculated with the following formula: RER = RIR_{post}/RIR_{pre}, where RER is the relative enhancement ratio, RIR_{post} is the postcontrast relative intensity ratio, and RIR_{pre} is the precontrast relative intensity ratio. Tumor enhancement was defined as high when the relative enhancement ratio was more than one, which meant that the tumor was enhanced more than the adjacent liver parenchyma, and as low when the relative enhancement ratio was less than one.

Evaluation of Immunohistochemical Staining Results

Immunostaining of the tumors and that of the adjacent liver parenchyma was compared in terms of staining patterns and stain intensities by the two previously described liver pathologists, independently and without knowledge of the MR imaging data. Disagreement was resolved with consensus. The results of immunohistochemical staining for tumors were determined by using the following three-point scale: score 0, negative or minimal; score 1+, positive to the same or lesser extent compared with the adjacent liver parenchyma; and score 2+, positive to a higher degree than the adjacent liver parenchyma (Figs E1, E2 [online]). Immunopositivity was determined by staining of the membrane of hepatocytes or tumor cells but not in terms of cytoplasmic reactivity, if present. MRP2 expression in tumors was assessed separately on canaliculi and the luminal membrane of pseudoglands.

Evaluation of Bile Pigment

The degree and the location of bile pigment of HCC were evaluated macroscopically on color images of the cut surface of the resected specimens and microscopically on sections stained with hematoxylin-eosin by means of its greenish color. Two authors (H.A. and K.W., with 8 years of experience in hepatobiliary surgery and 28 years experience in liver pathology, respectively) rated the degree of bile accumulation in consensus with the following three-point scale: score 0, negative; score 1+, focal; and score 2+, diffuse.

Statistical Analysis

In regard to statistical analysis of OATP1B1 and/or -1B3 and bile pigment, categories 1+ and 2+ were combined, although the evaluation data were collected on a three-point scale. In regard to statistical analysis of MRP2, overall expression was determined by combining the results for expression on canaliculi and pseudoglands. When the degrees of expression on the two structures were the same, the same score was assigned for the overall expression, and when the degrees of expression on the two structures were different, the higher score was applied as the overall expression. The Student *t* test was then used to compare the relative enhancement ratio between the two groups, specifically for the following: nodules with positive (score 1+ or 2+) versus negative or minimal (score 0) expression of OATP1B1 and/or -1B3, nodules with increased (score 2+) versus decreased (score 1+) overall expression of MRP2, and nodules with present (score 1+ or 2+) versus absent (score 0) bile pigment. Tumor sizes were also compared between nodules with high and low enhancement by using the Student *t* test. An analysis of variance was used for multigroup comparison, and when the results showed significant differences among groups, comparisons between groups were performed with the Scheffé post hoc test. A *P* value of less than .05 was considered to indicate a significant difference.

Results

Expression of OATP1B1 and/or -1B3

Basolateral expression in liver parenchyma was strong in the centrilobular area, moderate in the midzonal area, and absent in periportal hepatocytes (Fig E1a [online]), which is in agreement with the data in previous studies (18,19). Positive expression of OATP1B1 and/or -1B3 in HCC was observed in 14 (52%) nodules. The distribution of positive cells was broad and diffuse (Fig E1b [online]) in five nodules and focal and sparse (Fig E1c [online]) in nine nodules.

Expression of MRP2

Canalicular expression of MRP2 without zonal variation was observed in liver parenchyma (Fig E2a [online]). All HCC nodules were positive for MRP2, and the expression was localized either in the luminal membrane of pseudoglands (Fig E2b [online]) or in the canalicular membrane of tumor cells arranged in trabecular structures (Fig E2c, E2d [online]). Overall MRP2 expression was increased in 20 (74%) nodules and unchanged or decreased in seven (26%) nodules. Of the 20 nodules with increased expression, six nodules showed increased expression at the luminal membrane of the pseudoglands (Fig E2b [online]), and the remaining 14 nodules showed increased expression only at the canaliculi and decreased or negative expression in the luminal membrane of pseudoglands, if present (Fig E2c [online]).

Relative Enhancement Ratio of Tumors in Relation to Expression of Transporter Proteins and Bile Accumulation

The mean relative enhancement ratio for all nodules was 0.82. Nodules with positive expression of OATP1B1 and/or -1B3 showed a significantly higher relative enhancement ratio than did nodules with negative or minimal expression (mean, 0.94 and 0.68, respectively; $P = .002$) (Fig 1a). All five nodules with high enhancement expressed OATP1B1 and/or -1B3, whereas nine (64%) of 14 nodules with positive OATP1B1 and/or -1B3 expression showed low enhancement similar to that of the nodules with negative or minimal expression (Table 1). There was no significant difference in mean relative enhancement ratio between nodules with increased MRP2 expression and those with unchanged or decreased MRP2 expression (mean, 0.82 and 0.81, respectively; $P = .9$) (Fig 1b).

Figure 1

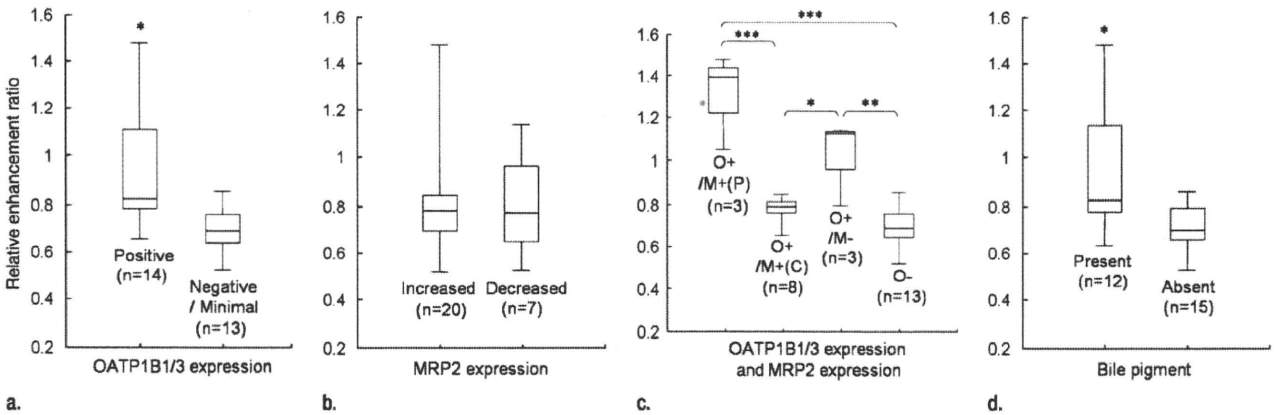

Figure 1: Box plots of relative enhancement ratios of nodules, indicating the median (horizontal line), the 75th (top of box) and 25th (bottom of box) quartiles, and the smallest and largest values (whiskers). **(a)** OATP1B1 and/or -1B3 expression. Mean values were significantly higher for nodules with positive expression than for nodules with negative or minimal expression. * = $P = .002$, Student *t* test. **(b)** MRP2 expression. Mean values were not significantly different for nodules with increased expression and nodules with unchanged or decreased expression ($P = .9$, Student *t* test). **(c)** OATP1B1 and/or -1B3 *(OATP1B1/3)* and MRP2 expression, with comparison of four groups of nodules classified by expression patterns of both OATP1B1 and/or -1B3 and MRP2. Mean values were significantly higher for the two groups: nodules with increased MRP2 expression at the luminal membrane of pseudoglands and nodules with decreased MRP2 expression, both combined with positive OATP1B1 and/or -1B3 expression (Scheffé post hoc test). * = $P = .047$, ** = $P = .002$, *** = $P < .001$. *O+* = OATP1B1 and/or -1B3 positive, *O–* = OATP1B1 and/or -1B3 negative, *M+(P)* = increased MRP2 expression at luminal membrane of pseudoglands, *M+(C)* = increased MRP2 expression only at canaliculi, *M–* = unchanged or decreased MRP2 expression. **(d)** Bile pigment. Mean values were significantly higher for nodules with bile pigment than for nodules without bile pigment. * = $P = .004$, Student *t* test.

Figure 2

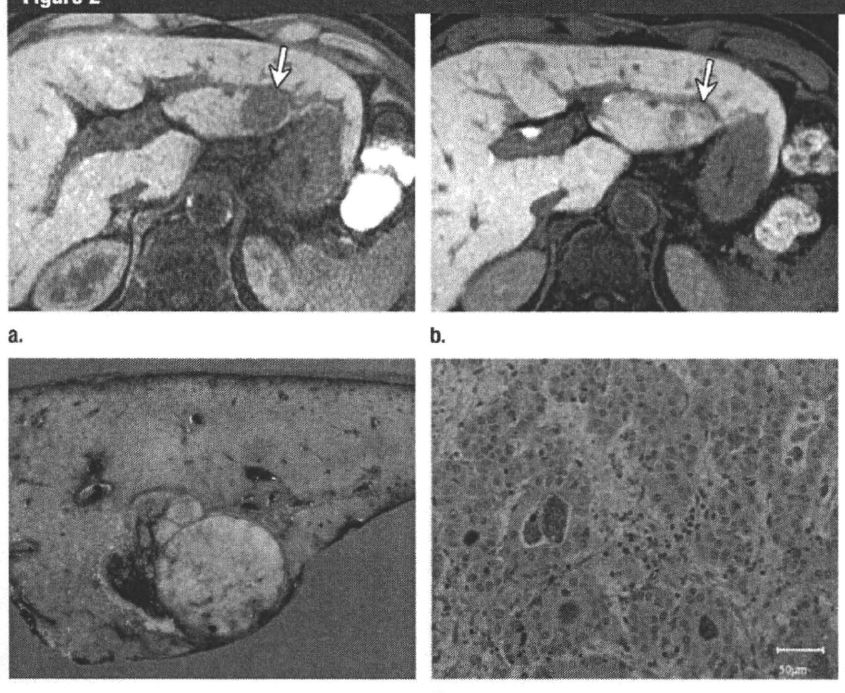

Figure 2: Moderately differentiated HCC with high hepatocyte-selective enhancement in 65-year-old man (Table 1, patient 1). **(a)** Precontrast MR image shows tumor (arrow, also on **b**). **(b)** Gadoxetic acid–enhanced hepatobiliary phase MR image shows that tumor had higher enhancement than did adjacent liver parenchyma. **(c)** Image shows that tumor had diffuse greenish color on cut surface. **(d)** Photomicrograph of section stained with hematoxylin-eosin shows bile pigment in lumina of pseudoglands. (Original magnification, ×20.) Immunohistochemical staining showed prominent expression of MRP2 in luminal membrane of pseudoglands (Fig E2b [online]). OATP1B1 and/or -1B3 expression was positive (not shown).

Ann Surg Oncol (2010) 17:3145–3154
DOI 10.1245/s10434-010-1150-9

Annals of
SURGICAL ONCOLOGY
OFFICIAL JOURNAL OF THE SOCIETY OF SURGICAL ONCOLOGY

ORIGINAL ARTICLE – HEPATOBILIARY TUMORS

Exploration of Potential Genomic Portraits Associated with Intrahepatic Recurrence in Human Hepatocellular Carcinoma

Nobuyoshi Kittaka[1], Ichiro Takemasa[1], Shigeto Seno[2], Yutaka Takeda[1], Shogo Kobayashi[1], Shigeru Marubashi[1], Keizo Dono[1], Koji Umeshita[1], Hiroaki Nagano[1], Hideo Matsuda[2], Morito Monden[1], Masaki Mori[1], and Yuichiro Doki[1]

[1]Department of Surgery, Gastroenterological Surgery, Graduate School of Medicine, Osaka University, Osaka, Japan; [2]Department of Bioinformatic Engineering, Graduate School of Information Science and Technology, Osaka University, Osaka, Japan

ABSTRACT

Background. Hepatocellular carcinoma (HCC) is a heterogeneous disease with recognized variability in virus infection, genetic features, and clinical outcome. To date, transcriptional profilings of HCC have been used to predict recurrence or survival/prognosis. However, there remains a challenge to identify specific genomic prints associated with HCC recurrence, which could lead to novel therapies or effective treatment. Here we examine the association between biological signals and intrahepatic recurrence using global gene expression profiles and powerful analytical methods.

Materials and Methods. Gene expression profiles were generated in 24 HCC patients with hepatitis B infections (B-type HCC) and 60 HCC patients with hepatitis C infections (C-type HCC). Gene set enrichment analysis (GSEA) was applied to the entire ranked gene lists related to early intrahepatic recurrence, based on "ideal discriminator method."

Results. GSEA revealed *Ribosomal Proteins* as a common regulatory pathway in B-type ($P < .001$) and C-type ($P = .003$) HCC recurrence. In addition, *Proteasome* ($P < .001$) and *Pentose Phosphate Pathway* ($P = .01$) were identified as specific pathways in each type of HCC recurrence, respectively.

Conclusions. Understanding these biologically common and different mechanisms related to intrahepatic recurrence in B-type and C-type HCC could be useful in the development of new therapeutic strategies in our fight against HCC.

Hepatocellular carcinoma (HCC) is the third major cause of cancer-related deaths in Japan, and about half a million new cases are diagnosed each year worldwide.[1] A major obstacle in the treatment of HCC is intrahepatic recurrence, which develops in 30–50% of patients who undergo hepatic resection. Therefore, intrahepatic recurrence limits the potential of surgery as a cure for HCC.[2] The major histopathological features that can be used to predict HCC recurrence are vascular invasion, degree of differentiation of the tumor, and multinodularity.[3]

In general, it is considered that cancer cell metastasis is a multistep, complex process including migration of detached cells from the primary tumor through the surrounding stroma, invasion of the cells into the circulatory system, extravasation, and arresting at distant secondary sites. In addition, metastatic cells have to undergo genetic and epigenetic changes to acquire their aggressive phenotypes.[4] For example, as clinical experience with HER-2 and epidermal growth factor receptor inhibition in breast cancer has illustrated, identification and selection of patients who are likely to respond to molecularly targeted therapies are critical to the prevention of HCC recurrence.[5,6] In this study, it was supposed that intrahepatic metastasis might have been triggered by cell migration

Electronic supplementary material The online version of this article (doi:10.1245/s10434-010-1150-9) contains supplementary material, which is available to authorized users.

First Received: 24 April 2009;
Published Online: 13 July 2010

I. Takemasa
e-mail: itakemasa@gesurg.med.osaka-u.ac.jp

based on the activation of molecular signaling pathways, and, if the inhibition of those pathways were possible, novel therapeutic targets for HCC recurrence might be identified and help the improvement of prognosis in HCC.

Gene-expression profiling has emerged as a powerful technique to identify tumor subtypes, prognostic signatures, and potential therapeutic targets in human cancer.[7,8] Comparisons of gene expression patterns between HCC with hepatitis B infection (B-type HCC) and HCC with hepatitis C infection (C-type HCC) has shown that HBV and HCV cause hepatocarcinogenesis through different mechanisms.[9] Several recent studies have employed the gene expression profiling to address the issue of HCC recurrence following resection of the primary lesion.[10–12] The challenge no longer lies in obtaining gene expression profiles, but rather in interpreting the results to gain insights into biological mechanisms and in identifying genetic determinants that are components of the specific regulatory pathways altered in B-type and C-type HCC recurrence. To date, a transcriptional approach to predicting HCC recurrence has been used to highlight the construction of molecular prediction systems and the functional genomics focused on classifier genes.[13,14] However, since then approaches focusing on classifier genes that exhibit differences between 2 states of interest have failed to detect biological mechanisms that are distributed across the entire network of genes and subtle mechanisms at the level of individual genes. Based on this background, we used a powerful analytical approach known as gene set enrichment analysis (GSEA) to identify the main regulatory pathways associated with early intrahepatic recurrence out of several biological mechanisms, as this approach can offer advantages over traditional analytical methods in identifying coordinately regulated gene sets versus differences in expression of single genes.[15,16] To understand the biological mechanisms of B-type and C-type HCC recurrence and design specific tailor-made therapeutic strategies for each type of HCC recurrence, it is essential to clarify the common and different potential regulatory pathways associated with intrahepatic recurrence caused by HBV and HCV infection, with a special focus on the entire genetic alterations between the early recurrence group and the nonrecurrence group.

MATERIALS AND METHODS

Tissue Samples

Samples from 84 HCC tissues and 7 normal livers free of virus infection were obtained with informed consent from patients who underwent hepatic resection at Osaka University Hospital from 1997 to 2006. The study protocol was approved by the Institutional Review Board for Human Use at the Graduate School of Medicine, Osaka University. Taking into consideration that invasion of tumor cells into the host tissue is regulated by the matrix microenvironment at the tumor/host-tissue interface, we sectioned sample tissues from peripheral region of specimens.[17] Tissue specimens for RNA isolation were stored at −80°C until use. The histopathological characterization of HCC was based on the Classification of the Liver Cancer Study Group of Japan. Table 1 lists the clinical and pathological features of the 84 cases of HCC. Patients were classified into 2 groups, those positive for HBs Ag (B-type HCC, $n = 24$) and those positive for HCV Ab (C-type HCC, $n = 60$); none were positive for both HBs Ag and HCV Ab. The early recurrence group represents patients who developed intrahepatic recurrences within 2 years after resection of the primary HCC, and the nonrecurrence group comprises patients with more than 2-year disease-free survival (DFS) time. In this study, we selected the patients who did not undergo neoadjuvant and adjuvant chemotherapy.

Extraction and Quality Assessment of RNA

The −80°C storing period of each specimen that we used for RNA isolation was less than 2 years. Total RNA was purified from tissue samples using TRIzol reagent (Invitrogen, San Diego, CA) as described by the manufacturer. The integrity of RNA was assessed on an Agilent 2100 Bioanalyzer and RNA 6000 LabChip kits (Yokokawa Analytical Systems, Tokyo, Japan). In this study, we used the samples with a RNA Integrity Number (RIN) above 7.0 for gene expression analysis. RNA extracts from 7 normal liver tissues were mixed together as the control reference.

Preparation of Fluorescently Labeled aRNA Targets and Hybridization

Extracted RNA samples were amplified with T7 RNA polymerase using the Amino Allyl MessageAmp aRNA kit (Ambion, Austin, TX) according to the protocol provided by the manufacturer. The quality of each Amino Allyl-aRNA sample was checked on the Agilent 2100 Bioanalyzer. Then 5 μg of control and experimental aRNA samples were labeled with Cy3 and Cy5, respectively, mixed and hybridized on an oligonucleotide microarray covering 30,336 human probes (AceGene Human 30 K; DNA Chip Research Inc. and Hitachi Software Engineering Co., Yokohama Japan). As reported previously, the experimental protocol is available at http://www.dna-chip.co.jp/thesis/AceGeneProtocol.pdf.[18,19] The microarrays were scanned on a ScanArray 4000 (GSI Lumonics, Billerica, MA).

TABLE 1 Clinical and pathological characteristics of 84 patients with HCC

	B-type HCC ($n = 24$)			C-type HCC ($n = 60$)		
	Nonrecurrence ($n = 6$)	Early recurrence ($n = 18$)	P value	Nonrecurrence ($n = 21$)	Early recurrence ($n = 39$)	P value
Sex			.14[b]			.75[b]
Male	4	17		17	29	
Female	2	1		4	10	
Age (years)			.99[a]			.26[a]
Mean	57.8	57.9		67.2	69.3	
SD	8.1	9.3		7.9	5.9	
AFP			.024[b]			.69[b]
<400 ng/mL	6	8		18	35	
≥400 ng/mL	0	10		3	4	
Edmondson grade			.061[b]			.025[b]
I, II	5	6		18	22	
III, IV	1	12		3	17	
Tumor size			.28[b]			.24[b]
<5 cm	6	12		20	32	
≥5 cm	0	6		1	7	
Venous invasion			.99[b]			.41[b]
+ve	0	2		1	5	
−ve	6	16		20	34	
CLIP score			.28[b]			.14[b]
0, 1	6	12		20	31	
≥2	0	6		1	8	

CLIP score The cancer of the Liver Italian Program score

[a] By t test

[b] By Fisher exact probability test

All P values are for comparison of nonrecurrence and early recurrence groups

Analysis of Microarray Data

Signal values were calculated using DNASIS Array Software (Hitachi Software Inc., Tokyo). Following background subtraction, data with low signal intensities were excluded from further investigation. In each sample, the Cy5/Cy3 ratio values were log-transformed. Then, global equalization to remove a deviation of the signal intensity between whole Cy3- and Cy5-fluorescence was performed by subtracting the median of all log (Cy5/Cy3) values from each log (Cy5/Cy3) value. Genes with missing values in more than 20% of the samples were excluded from further analysis. A total of 16,396 genes out of 30,336 remained.

Study Outline and Ideal Discriminator Method

In order to list all genes according to their expression levels in the early recurrence group, a heuristic method based on Pearson correlation ("ideal discriminator method") was performed (an outline of this method is shown in Supplementary Fig. 1).[20,21] An ideal discriminator is defined as a theoretical gene that is maximally expressed in all early recurrence group samples and minimally expressed in all nonrecurrence group samples, and the Pearson correlation coefficient between each gene and the ideal discriminator is calculated. The Pearson correlation coefficient between the ideal discriminator $I = \{I_i\}$ and a vector of gene expression values $x = \{x_i\}$ is given by,

$$\text{Pearson Correlation Coefficient} = \frac{\sum_{i=1}^{n} (I_i - \bar{I})(x_i - \bar{x})}{\sqrt{\sum_{i=1}^{n} (I_i - \bar{I})^2} \sqrt{\sum_{i=1}^{n} (x_i - \bar{x})^2}}$$

where $\bar{x}$ and $\bar{I}$ are the average of $I = \{I_i\}$ and $x = \{x_i\}$, respectively.

Moreover, permutation tests are performed by randomly sampling half samples from the early recurrence group and nonrecurrence group in order to evaluate whether such correlation coefficient can be found by chance. All genes are sorted by the average of the correlation coefficient resulting from permutations (the distribution of the average of correlation coefficient is shown in Supplementary Fig. 2). The genes with higher average of correlation coefficients relative to the ideal discriminator could be regarded as the genes that are expressed stably high in the early recurrence group and stably low in the nonrecurrence group. To evaluate the predictability of the discriminator genes, leave-one-out cross validation was performed based on the signal-to-noise ratio and weighted vote algorithm.[22]

Leave-One-Out Cross-Validation Procedure

At one time, we took one sample out and calculated signal-to-noise ratio that is,

$$p_i = \frac{\mu_1 - \mu_2}{\sigma_1 + \sigma_2}$$

where $[\mu_1, \sigma_1]$ and $[\mu_2, \sigma_2]$ denote the means and standard deviations of gene i for the samples in the recurrence and nonrecurrence) for each gene using the remaining samples. Then, we predicted the outcome of the sample we left out, incrementing the number of discriminator genes. In weighted voting, the magnitude of the vote is $p_i v_i$, where p_i is a signal-to-noise ratio of gene i and

$$v_i = \left| x_i - \frac{(\mu_1 - \mu_2)}{2} \right|$$

reflects the deviation of the expression level in the sample from the average of μ_1 and μ_2 (x_i represents the expression level of gene i in the sample we left out). The votes for each class are summed, and the sample is assigned to the class with the higher total vote. This procedure was repeated until each of the samples was left out once.

Gene Set Enrichment Analysis

GenMAPP 2.1 and GSEA 2.0.1 (a publicly available desktop application from the Broad Institute, at http://www.broad.mit.edu/gsea/software/software_index.html) were used to assess significantly regulated pathways in the two data sets (B-type and C-type HCC recurrence).[15,23] In GenMAPP database, a total of 138 pathways were applied for gene set size filters (min = 15, max = 500), whereas the remaining 67 gene sets were used in GSEA. The enrichment score (*ES*) of a gene set *S* characterizes whether the set of genes is randomly distributed across the list or falls mainly at the bottom or top of the list *L*. The null hypothesis that a gene set *S* randomly distributes across the ranked gene list *L* was tested with Kolmogorov–Smirnov test, with the statistical significance value (nominal *P* value) estimated through 1000 random permutations of the phenotype label. The gene sets with a high significance ($P < .05$) of enrichment are considered important in separating the distinct phenotypes. To extract the core members of high scoring gene sets that contribute to the *ES*, the leading-edge subset is defined as those genes in the gene set *S* that appear in the ranked list *L* at, or before, the point where the running sum reaches its maximum deviation from zero.

Classification Based on Principal Component Analysis

Principal Component Analysis (PCA) is a mathematical technique that reduces the effective dimensionality of gene expression profile without significant loss of information. The first principal component (PC1) accounts for as much of the variability in the data as possible; it is taken to be along the direction with the maximum variance. In this study, we performed PCA-based classification of patients using the expression profile of leading-edge subset genes. Depending on whether the value of PC1 is greater than 0 or not, patients were divided into 2 groups of high or low activated in the corresponding pathway. Then, the Fisher exact probability test was performed in order to investigate the correlations between these groups and surgical pathology.

RESULTS

Prediction of Early Intrahepatic Recurrence of HCC with Leave-One-Out Cross Validation and Evaluation of Discriminator Genes

We performed ideal discriminator method with 500 permutations to the 2 data sets (B-type HCC recurrence [$n = 18$] and nonrecurrence [$n = 6$], and C-type HCC recurrence [$n = 39$] and nonrecurrence [$n = 21$]). All 16,396 genes were rank-ordered based on the average of the correlation coefficient to the ideal discriminator (detailed data not shown). In each design set, HCC recurrence was predicted using full genes based on a WV algorithm with a leave-one-out cross-validation approach (accuracy curves of each type of HCC are shown in Fig. 1a,b; sensitivity, specificity, positive predicted values, and negative predicted values are shown in Supplementary Fig. 3). The 101 discriminator genes marked top accuracy (100%) in B-type HCC. The 119 discriminator genes marked top accuracy (91.7%) in C-type HCC. The expression levels of the discriminator genes with top accuracy that were overexpressed in B-type and C-type HCC are shown in Fig. 1c, d, respectively (detailed information is shown in Supplementary Tables 1 and 2). Next, we examined whether or not 101 discriminator genes derived from B-type HCC could subdivide C-type HCC into 2 subtypes (early recurrence and nonrecurrence) and whether or not 119 discriminator genes derived from C-type HCC could subdivide B-type HCC into 2 subtypes (early recurrence and nonrecurrence). The results showed no clear division of these subtypes (data not shown). In addition, comparison of the highly expressed discriminator genes with top accuracy in each type of HCC did not identify commonly expressed genes.

Identification of Characteristic Genomic Pathways Associated with Early HCC Recurrence Using GSEA

Having defined the differentially expressed profiles of B-type and C-type HCC recurrence, the challenge was to